RAA 2019 Vol. **19** No. **8**, 107(8pp) doi: 10.1088/1674–4527/19/8/107

http://www.raa-journal.org *http://iopscience.iop.org/raa*

***R**esearch in*
***A**stronomy and*
***A**strophysics*

Period investigation of Algol systems TZ Eri and TU Her

Zhi-Hua Wang[1,2,3,4], Li-Ying Zhu[1,2,3,4], Lin-Jia Li[1,2,3] and Xiao-Man Tian[1,2,3,4]

[1] Yunnan Observatories, Chinese Academy of Sciences, Kunming 650216, China; *wzh@ynao.ac.cn*
[2] Key Laboratory for the Structure and Evolution of Celestial Objects, Chinese Academy of Sciences, Kunming 650216, China
[3] Center for Astronomical Mega-Science, Chinese Academy of Sciences, Beijing 100101, China
[4] University of Chinese Academy of Sciences, Beijing 100049, China

Received 2018 December 20; accepted 2019 March 1

Abstract TZ Eri and TU Her are both classic Algol-type systems (Algols). By observing and collecting times of minimum light, we constructed the $O-C$ curves for the two systems. The long-time upward and downward parabolas shown in these diagrams are considered to be the result of the combination of mass transfer and angular momentum loss. The secular orbital period change rates are $dP/dt = 4.74(\pm0.12) \times 10^{-7}$ d yr^{-1} and $dP/dt = -2.33(\pm0.01) \times 10^{-6}$ d yr^{-1}, respectively. There are also cyclic variations in their $O-C$ curves which might be caused by the light-travel time effect (LTTE). A circumbinary star may exist in the TZ Eri system with a mass of at least $1.34\ M_{\odot}$, while there are possibly two celestial bodies that almost follow a $2:1$ resonance orbit around the TU Her binary pair. Their masses are at least $2.43\ M_{\odot}$ and $1.27\ M_{\odot}$.

Key words: stars: binaries: close — stars : binaries: eclipsing — stars: individual (TZ Eri, TU Her)

1 INTRODUCTION

Classic Algols are the semi-detached interacting binaries composed of a main-sequence primary and a lobe-filling evolved secondary component. If the mass and angular momentum are conservative, their period will increase with the mass transfer from the secondary to the primary component. However, both increasing and decreasing period changes are found in Algol systems. In general, Algols show EA-type light variations with relatively deep primary eclipse. Their light variations were noticed earlier than those of other types of eclipsing binaries, so they have a relatively long observational history. Many of them have a record of eclipse times of about 100 years ago. The long spanning data are of benefit for the period investigation. In the present paper, we investigated the period variation of the two classical Algols TZ Eri, and TU Her. Both of them have a long observational history.

TZ Eri (α_{2000} = 04:21:40.3, δ_{2000} = –06:01:09.20) was first detected as an Algol-type system by Hoffmeister (1929). Soon afterwards, Cannon (1934) determined its spectral type to be F. Later, Barblan et al. (1998) classified this target as A5/6 V for the primary star, and K0/1 III for the secondary star, and they obtained accurate physical parameters such as the masses ($1.97\ M_{\odot}$ and $0.37\ M_{\odot}$) and the radii ($1.69\ R_{\odot}$ and $2.60\ R_{\odot}$), based on its multi-color complete light curves and radial velocity curves. The observed emission lines are time variant before, during and after the eclipse (Kaitchuck & Honeycutt 1982; Vesper et al. 2001), so a possible transient disc may surround the primary star. Pulsation may also exist in this system by analyzing the small amplitude variations in the out-eclipse light curves (Liakos et al. 2008). The orbital period changes of TZ Eri were analyzed by Zasche et al. (2008), showing a secular increasing trend of orbital period. In addition, these authors found a third component with a mass of at least $1.3\ M_{\odot}$.

The orbital period of TU Her (α_{2000} = 17:13:35.4, δ_{2000} = 30:42:36.04) in the VSX database is 2.2669385 days. It is an F0/F5 + M1 spectral type system. Stewart (1915) reported the first eclipse data of this target. From that time on, plenty of observational results have been published by many researchers i.e. Nijland (1931), Todoran

Table 1 Parameters of TZ Eri and TU Her

Target	$P_{\rm orb}$ (d)	m_1 ($M_\odot$)	m_2 ($M_\odot$)	r_1 ($R_\odot$)	r_2 ($R_\odot$)	i (°)	A ($R_\odot$)	f_1 [%]
TZ Eri	2.606111	1.97	0.37	1.69	2.6	86.7	10.57	30.4
TU Her	2.266954	1.43	0.57	1.60	2.7	87.0	9.15	38.0

Notes: $P_{\rm orb}, m_1, m_2, r_1, r_2, i, A$ and f_1 are the orbital period of the eclipsing system, masses of the primary and secondary stars, radii of the primary and secondary stars, the orbital inclination, the semi-major axis and the filling factor of the primary star.

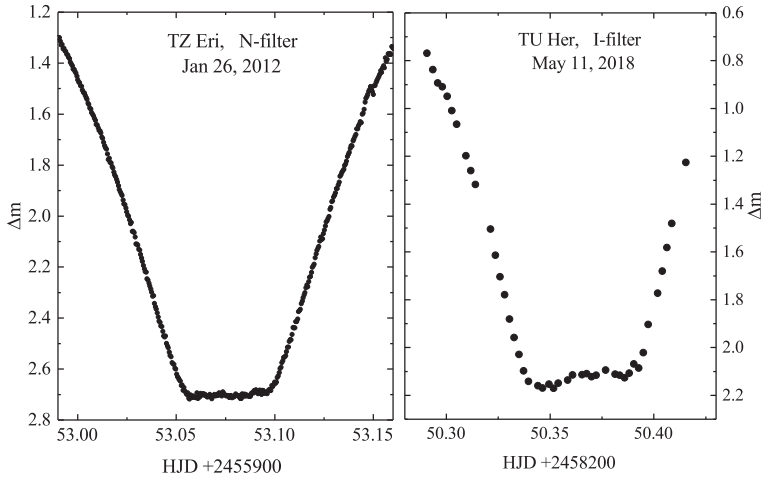

Fig. 1 Light curves during eclipse for TZ Eri (*left*) observed on 2012 Jan 26, and for TU Her (*right*) observed on 2018 May 11 by 60 cm telescope.

& Popa (1967), Mallama (1980), Brancewicz & Dworak (1980), Diethelm (2003), Samolyk (2010), etc. According to the result of Barblan et al. (1998) and Budding et al. (2004), the absolute parameters were obtained and are listed in Table 1. Similar to TZ Eri, this system was also found to exhibit a possible transient accretion disc by determining the Hβ–Hγ emission lines (Kaitchuck et al. 1985) and pulsation phenomenon by analyzing the tiny variations on the light curves (Lampens et al. 2004). Li et al. (1987) and Qian (2000a) made a brief investigation on the orbital shrinkage of this system. Recently, Khaliullina (2018) noticed that magnetic activity and a third-body is needed to analyze the periodic variations.

2 PHOTOMETRIC OBSERVATIONS

The observations for TZ Eri and TU Her were carried out with 1.0 m and 60 cm telescopes at Yunnan Observatories (YNOs, $102.804°$E, $25.032°$N) in 2007, 2012, 2016 and 2018. In 2007, the PI 1024 TKB CCD photometric system attached to a 1.0 m reflecting telescope was used. In other years, Andor DW 436 2K CCD systems attached to 1.0 m and 60 cm telescopes were used. Both telescopes are equipped with standard Johnson-Cousin-Bessel BVR_cI_c filters. We use the aperture photometry package PHOT (which measures magnitudes for a list of stars) in IRAF to reduce the observed images. Several new eclipsing profiles were obtained.

Figure 1 shows two eclipsing profiles observed on 2012 January 26 for TZ Eri and on 2018 May 11 for TU Her respectively.

With these photometric observations, five timings of minimum were derived on 2007 March 5, 2007 October 23, 2012 January 26, 2016 November 19, and 2018 May 11, respectively. They are all summarized in Table 2.

3 ORBITAL PERIOD ANALYSIS

In an eclipsing binary system, the observed primary eclipsing times of every epoch were usually recorded as O (or T_O), and the time difference between two adjacent eclipse times is the orbital period. If this period is constant and precise, the following transit times can be calculated and predicted, which are usually marked with C (or T_C). But the orbital period of a binary system usually changes slightly. Therefore, there is a difference between O and C in each orbital cycle. The value of $O-C$ can be resolved by Taylor

series expansion, and the plotted $O-C$ diagram reflects the orbital period changes.

To describe the $O-C$ curve, the combination of a quadratic term and an additional term is usually used, and written as

$$O-C=\Delta T_0+\Delta P_0 E+\frac{1}{2}P'(0)E^2+\tau\ , \quad (1)$$

where ΔT_0 and ΔP_0 are tiny corrections for the initial epoch and the orbital period, $P'(0)$ is the linear change of the orbital period (days/cycle), and τ is an additional term.

Remarkable works of Lanza (2005, 2006) and Liao & Qian (2010) provide the basis for the interpretation of the cyclic changes with the light-travel time effect (LTTE). Many people have reported this phenomenon (e.g., Gies et al. (2012), Martin et al. (2015), Carter et al. (2011), Zhu et al. (2013, 2016), Guo et al. (2018), Tian et al. (2018)). The LTTE was first introduced by Irwin (1952), where an analytic formula for the last-term in Equation (1) can be written as follows,

$$\tau=K\Big[(1-e_3^2)^{0.5}\sin E_a\cos\omega+\cos E_a\sin\omega\Big]\ , \quad (2)$$

where $K=\frac{a_{12}\sin i^*}{c}(1-e_3^2\cos^2\omega)^{0.5}$ is the oscillating amplitude of τ, e_3 is the eccentricity of the third body, i^* is the inclination of the third-body orbit, ω is the longitude of the periastron, a_{12} is the semi-major axis of the eclipsing pair orbiting around the common mass center of the whole system, c is the speed of light in vacuum and E_a is the eccentric anomaly.

The elliptical Kepler orbital equation established a connection through the mean anomaly (M_a) between eccentric anomaly (E_a) and the observed times of minimum light, $M_a=E_a-e_3\sin E_a=2\pi(t-T)/P_3$, where M_a is the mean anomaly, P_3 is the anomalistic period of additional bodies, t is the time of observed light minimum, and T is the periastron time. Considering that the above equation is a transcendental equation, E_a has to be expanded as a Bessel's series,

$$E_a=M_a+\sum_{n=1}^{+\infty}\frac{2}{n}J_n(nE)\sin(nM_a)\ , \quad (3)$$

where

$$J_n(nE)=\sum_{k=0}^{+\infty}(-1)^k\frac{1}{k!\Gamma(n+k+1)}\left(\frac{nE}{2}\right)^{n+2k}\ . \quad (4)$$

Then with the method of least-squares fitting and the Levenberg-Marquardt algorithm, the fitting curves and orbital parameters are finally obtained.

Table 2 New Light Minima for TZ Eri and TU Her

Target	HJD	Error	p/s	Filter	Telescope
TZ Eri	2454397.22538	±0.00004	p	*V*	1 m
TZ Eri	2455953.07619	±0.00009	p	*N*	60 cm
TZ Eri	2457712.20115	±0.00031	p	$BV(RI)_c$	60 cm
TU Her	2454165.31190	±0.00050	p	R_c	1 m
TU Her	2458250.36353	±0.00098	p	$V(RI)_c$	60 cm

3.1 Period Analysis of TZ Eri

We collected all the available data from the *ocgateway (var.astro.cz/ocgate/)* and from literature by many researchers, e.g. Perova (1975), Mallama (1980) and Wolf & Kern (1983). Along with our observations, a total of 85 visual data and 26 photoelectric and CCD data were compiled. By using the orbital period from the *ocgateway*, it is easy to write out the following linear ephemeris,

$$\mathrm{Min.I}=\mathrm{HJD2457761.72030}+2.606111\times E\ , \quad (5)$$

from which we could calculate the epoch, $O-C$ value and their residuals.

The open circles in Figure 2 refer to the visual data, and the dots stand for the CCD and photoelectric observations. It is obvious that the changes of the $O-C$ curve are smooth and continuous. The upper panel, $(O-C)_1$, shows all the variations which cannot be fitted by a single parabola but by a combined curve. After subtracting the open-up parabola, the residuals $(O-C)_2$ are plotted in the middle panel showing a sinusoidal-like variation with an amplitude of about 0.43 days. These data can be well fitted through the LTTE method. The final residuals $resi$ are plotted in the bottom panel. It should be noted that during the data fitting a weight of 1 for the open circles and 10 for the dots were set.

The new quadratic ephemeris of TZ Eri is then written as

$$\begin{aligned}\mathrm{Min.I}=&\mathrm{HJD2457761.69279}+2.6061267\times E\\&+1.6925\times10^{-9}\times E^2\ .\end{aligned} \quad (6)$$

3.2 Period Analysis of TU Her

We reanalyzed this target by adding our own observations and other photometric observations from many articles, such as Todoran & Popa (1967), Mallama (1980), etc. In total, 260 visual and photographic data and 40 CCD observational data were collected and compiled. The linear ephemeris is written as follows,

$$\mathrm{Min.I}=\mathrm{HJD2456801.7769}+2.266954\times E. \quad (7)$$

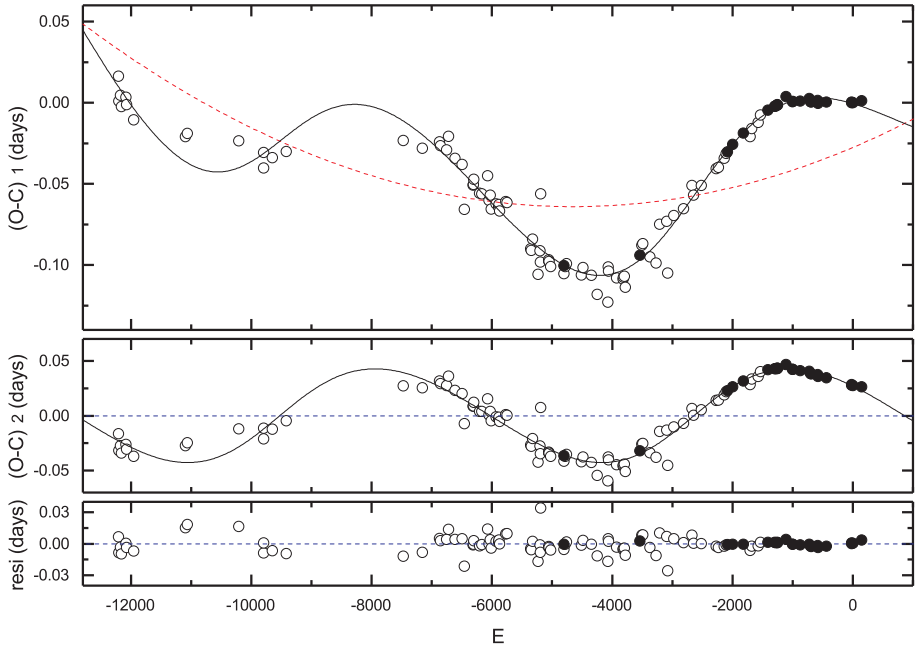

Fig. 2 *The upper panel*: $(O-C)_1$ curve of TZ Eri. *The middle panel*: $(O-C)_2$ curve. *The bottom panel*: the residuals (resi). The *open circles* refer to visual observational data and the dots to photoelectric and CCD observations.

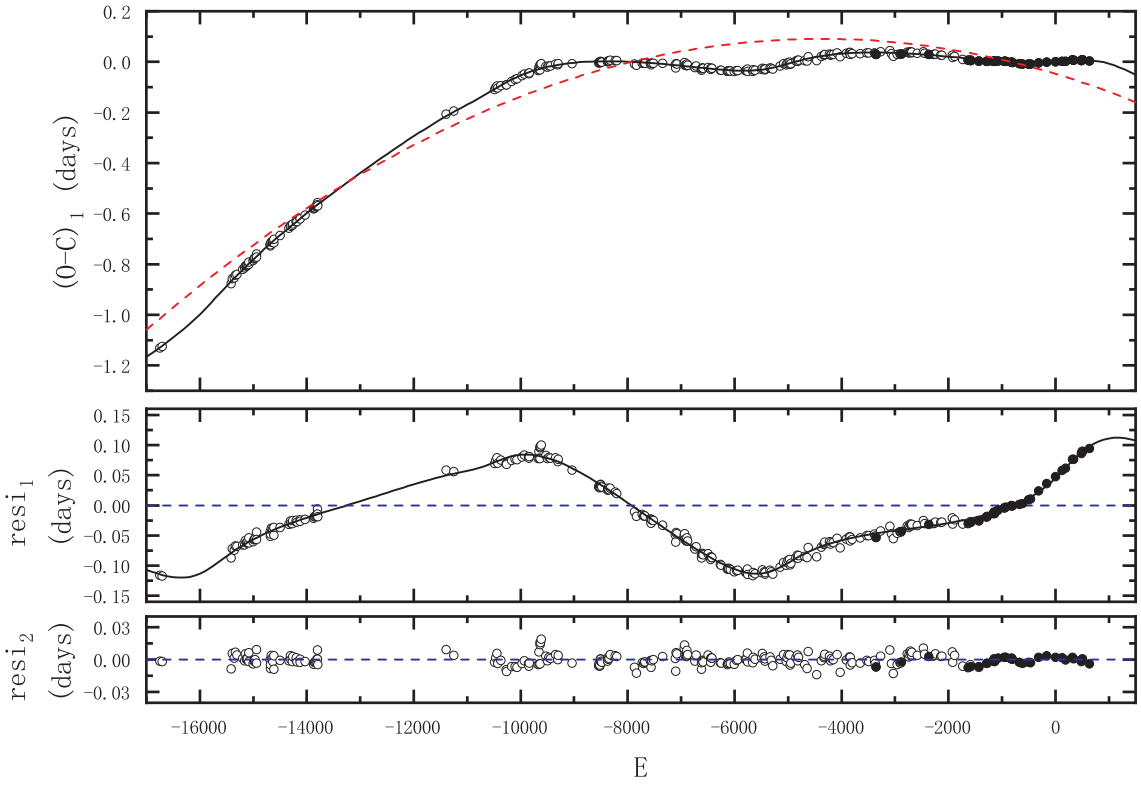

Fig. 3 *The upper panel*: $(O-C)_1$ curve of TU Her. *The middle panel*: the residuals from the parabolic fit. *The bottom panel*: the final residuals computed from the above fittings. The *open circles* refer to visual and photographic data and the *dots* to CCD observations.

Similar to the TZ Eri system, Equations (1) and (2) were used to fit the $O-C$ data. The open circles in Figure 3 represent visual and photographic data, and the dots are the CCD observations. The weights of the low-precision and high-precision data are set as 1 and 10 respectively. An open-down solid parabolic fitting line and a complicated curve were plotted in the upper panel of Figure 3. After removing the para-curve, the complex solid line was plot-

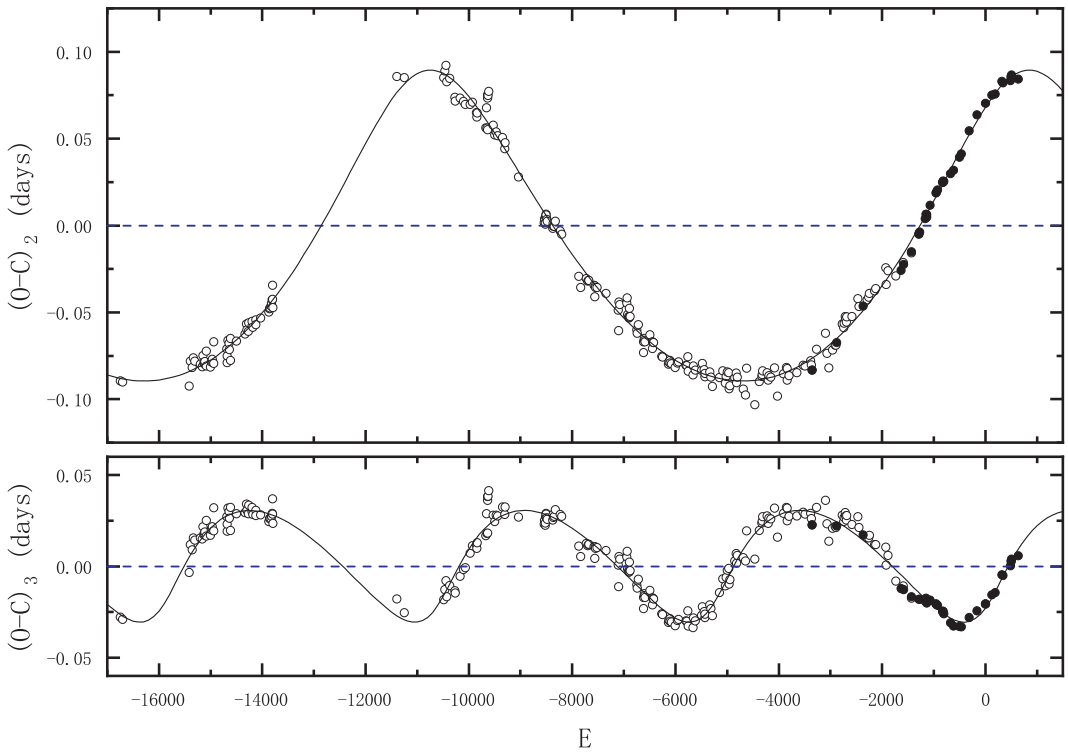

Fig. 4 Two cyclic changes of TU Her both derived from resi_1. *The upper panel*: $(O-C)_2$ of one cyclic variation. *The lower panel*: $(O-C)_3$ of another cyclic variation. The *open circles* refer to visual and photographic data and the *dots* to CCD observations.

ted in the resi_1 panel. This complex curve cannot easily be processed with a single sinusoidal fitting.

Assuming that such residuals are due to the LTTE caused by two additional bodies, the resi_1 data in Figure 3 could be well fitted by the model,

$$\mathrm{resi}_1 = (O-C)_1 - \Delta T_0 - \Delta P_0 E - \frac{1}{2}P'(0)E^2. \quad (8)$$

The two cyclic variations in Figure 4 are derived from resi_1. The data in Figure 4 are calculated from the following equations,

$$\begin{aligned}(O-C)_2 =& \mathrm{resi}_1 - K_4\Big[(1-e_4^2)^{0.5}\sin E_a\cos\omega_4 \\ &+ \cos E_a \sin\omega_4\Big]\,,\end{aligned} \quad (9)$$

and

$$\begin{aligned}(O-C)_3 =& \mathrm{resi}_1 - K_3\Big[(1-e_3^2)^{0.5}\sin E_a\cos\omega_3 \\ &+ \cos E_a \sin\omega_3\Big]\,,\end{aligned} \quad (10)$$

where K_3, K_4, e_3, e_4, ω_3, and ω_4 are parameters of the third and fourth stars.

The amplitudes of these two variations are 0.090 days and 0.032 days. The two cyclic variations shown in the $(O-C)_2$ and $(O-C)_3$ diagrams are vibrating at large amplitudes. Their oscillation periods are 11 593 cycles and 5319 cycles. It is probable that no other effective signals could be extracted from the final residuals (resi_2).

The new quadratic ephemeris of TU Her is obtained,

$$\begin{aligned}\mathrm{Min.I} =& \mathrm{HJD}2456801.72937 + 2.2668907\times E \\ &- 7.225\times10^{-9}\times E^2.\end{aligned} \quad (11)$$

4 DISCUSSION AND CONCLUSIONS

4.1 Secular Orbital Evolution

Long term changes of the orbital period in Algol-type close binary systems are very common phenomena. The orbital period of some Algols present a secular increasing tendency, such as systems of S Equ (Qian & Zhu 2002), UW Vir (Zhang et al. 2009) and AI Dra (Liao et al. 2016, while other Algols show decreasing behaviors of the orbital period, e.g., Qian (2000b, 2001a,b, 2002); Zhu et al. (2009); Erdem & Öztürk (2014) and Wang & Zhu (2016). The two targets reported in this work are typical examples. TZ Eri is an Algol-type binary system with the orbital period increasing at a rate of $dP/dt = 4.74(\pm0.12)\times 10^{-7}$ d yr^{-1}. TU Her, however, has a downward parabolic change on the $O-C$ curve, which indicates that the orbital period is decreasing at a rapid rate of $dP/dt = -2.33(\pm0.01)\times10^{-6}$ d yr^{-1}, or -7.225×10^{-9} d cycle^{-1}, and it is in accordance with the numerical value $-7.7\times$

Table 3 Parameters Based on $O-C$ Analysis

Parameter	TZ Eri	TU Her	
K (d)	0.043(±0.001)	0.090(±0.001)	0.032(±0.001)
$e_{3,4}$	0.15 (±0.04)	0.364(±0.027)	0.401(±0.030)
$a_{12}\sin i^*$ (AU)	7.56 (±0.25)	15.59(±0.73)	5.94 (±0.34)
$P_{3,4}$ (d)	17946(±173)	26281(±204)	12058(±57)
$f(m_{3,4})$ $(M_\odot)$	0.178(±0.018)	0.729(±0.104)	0.191(±0.033)
$m_{3,4(\min)}$ $(M_\odot)$	1.34 (±0.01)	2.43 (±0.08)	1.27 (±0.05)
$a_{3,4(\max)}$ (AU)	13.18(±1.31)	12.85(±1.78)	9.35 (±1.18)
ΔT_0[cor]	–0.02751(±0.00165)	–0.04753(±0.00296)	
ΔP_0[cor]	1.57(±0.07)×10^{-5}	–6.33(±0.08)×10^{-5}	
$P'(0)$ (d cycle^{-1})	3.385(±0.115) ×10^{-9}	–1.445(±0.008)×10^{-8}	

10^{-9} d cycle^{-1} in the ephemeris in the previous work by Khaliullina (2018).

The secular orbital evolution could have been caused by complex physical mechanisms. The first consideration is the simple and conservative evolutionary model in a classic Algol-type binary system. Mass is transferring through the first Lagrange point (L_1) from the less massive star to the more massive star. The orbital period of the double stars will naturally increase. However, the evolution of binary systems is generally non-conservative. In this case, the mass and angular momentum continually escape from the central binary stars leaving the binary stars with a decreasing orbital period. For instance, circumbinary disc or matter possibly exists around a binary system, extracting angular momentum from the central pair and thus reducing the orbital period. This physical process was proved to be an effective way of shrinking the orbit of Algol-type binaries (Chen et al. 2006) and detached binaries (Chen & Podsiadlowski 2017). According to Tout & Eggleton (1988) and Tout & Hall (1991), the long-term behavior of the orbital period in the $O-C$ curves should be a composite result of mass transfer, and mass and angular momentum loss. If the orbital period change caused by mass transfer is larger than by that of angular momentum loss (AML), then the period will increase as seen in the case of TZ Eri. Otherwise, the AML is expected to dominate the secular orbital evolution and the orbital period shrinks as in the TU Her binary system.

4.2 Cyclic Orbital Evolution

In an eccentric orbital system, the projected radius $a_{12}\sin i^*$ of the eclipsing binary system rotating around the outer common mass center could be calculated with the equation $a_{12}\sin i^*(1-e_3^2\cos^2\omega)^{0.5}=cK$. The mass function can be written as follows

$$f(m_3)=\frac{4\pi^2}{GP_3^2}(a_{12}\sin i^*)^3 = \frac{(m_3\sin i^*)^3}{(m_1+m_2+m_3)^2}\ , \tag{12}$$

where G is the gravitational constant, P_3 is the period of the third body, m_1 and m_2 are masses of the primary and secondary components in the binary pair respectively, and m_3 is the mass of the additional third body. From the above, we can estimate the mass function and the mass of the third body. Furthermore, in the center-of-mass frame $m_3a_3=(m_1+m_2)a_{12}$. Then the orbital radius of the third body (a_3) can be figured out. The fitting parameters of the $O-C$ diagrams for these two targets are listed in Table 3.

In the $O-C$ curve of the TZ Eri system, the sinusoidal like variation can be well fitted through the LTTE model where a possible third star is orbiting around the central binaries with an eccentricity equal to 0.15. The orbital period of the outer star is 49.13 years. The minimum mass is about 1.34 solar mass, and the maximum orbital semi-axis is about 13.18 AU when its orbital plane is coplanar with the orbiting plane of the inner binary. Our data span is nearly a dozen years longer than that of Zasche et al. (2008). The added observational data accords with the variation trend of the earlier observations, and more or less confirms the former researchers' result. The new eccentricity is a little different and has been updated.

For the TU Her system, the curve of the $O-C$ residuals (the lower panel in Fig. 3) is complex and interesting. However, our fitting result shown in Figures 3 and 4 is neat and plausible, and the two cyclic variations extracted from the residuals resi_1 both use the eccentric LTTE model. That means two stars are circling around the inner binary pair, making up a hierarchical quadruple system. Their eccentricities are 0.364 and 0.401. They almost run in a 2:1

resonance orbit for their orbital period are respectively 26 281(±204) days and 12 058(±57) days. Their masses are estimated to be at least 2.43 $M_\odot$ and 1.27 $M_\odot$. The maximum orbital semi-axes are 12.85 AU and 9.35 AU. The third bodies are all in stellar-level, but their spectral lines have not been published, which may indicate that they are compact stars. This is the approach to the result computed by Khaliullina (2018), whereas he finally interpreted that the LTTE is able to explain only one of the cyclic variations.

Applegate (1992) illustrated the cyclic modulation on the $O-C$ variation caused by magnetic activities of late-type stars in close binary systems. The quadrupole moment variation ΔQ is figured out by the following formula,

$$\frac{\Delta P}{P} = -9\frac{\Delta Q}{m_2 A^2}\ , \tag{13}$$

where the separation A is derived from the simplified Kepler's third law, $(m_1+m_2)P_{\rm orb}^2 = 0.0134A^3$. According to Rovithis-Livaniou et al. (2000), $\Delta P = K_{\rm mod}\sqrt{2[1-\cos(2\pi P_{\rm orb}/P_*)]}$, where $K_{\rm mod}$ is the amplitude, and P_* is the period of the sinusoidal function. By using a sinusoidal fitting, the cyclic period vibration rates for TZ Eri and TU Her are $\Delta P/P = 1.48\times10^{-5}$ and $\Delta P/P = 2.09\times10^{-5}$. So, the quadrupole moment variation (ΔQ) for the two late-type stars are separately 6.54×10^{50} g cm^2 (star 2 in TZ Eri) and 1.07×10^{51} g cm^2 (star 2 in TU Her), whereas the typical ΔQ should be on the order of $10^{51}-10^{52}$ g cm^2 (Lanza & Rodonò 1999). So, the magnetic activity is possibly suitable for TU Her but not for TZ Eri. Additionally, the cyclic variations in Figure 4 are strictly periodic with more than one cycle, and are well fitted by the LTTE model. Thus we are more convinced by the explanation of the LTTE model.

Orbital period variations in semi-detached Algols are very interesting but not clear yet. The period analysis for each Algol target is far from enough. With the accumulation of the analyses for these samples, statistical works will be able to be carried out. In order to uncover the nature of the secular opposite orbital evolutionary behaviors in Algol-type systems, both theoretical and statistical works are needed in the future.

Acknowledgements This work is partly supported by the National Natural Science Foundation of China (Nos. 11573063 and 11611530685), the Key Science Foundation of Yunnan Province (No. 2017FA001), the CAS "Light of West China" Program and the CAS Interdisciplinary Innovation Team.

References

Applegate, J. H. 1992, ApJ, 385, 621
Barblan, F., Bartholdi, P., North, P., Burki, G., & Olson, E. C. 1998, A&AS, 132, 367
Brancewicz, H. K., & Dworak, T. Z. 1980, Acta Astronomica, 30, 501
Budding, E., Erdem, A., Çiçek, C., et al. 2004, A&A, 417, 263
Cannon, A. J. 1934, Harvard College Observatory Bulletin, 897, 12
Carter, J. A., Fabrycky, D. C., Ragozzine, D., et al. 2011, Science, 331, 562
Chen, W.-C., Li, X.-D., & Qian, S.-B. 2006, ApJ, 649, 973
Chen, W.-C., & Podsiadlowski, P. 2017, ApJ, 837, L19
Diethelm, R. 2003, Information Bulletin on Variable Stars, 5438
Erdem, A., & Öztürk, O. 2014, MNRAS, 441, 1166
Gies, D. R., Williams, S. J., Matson, R. A., et al. 2012, AJ, 143, 137
Guo, D. F., Li, K., Hu, S. M., & Chen, X. 2018, PASP, 130, 064201
Hoffmeister, C. 1929, Astronomische Nachrichten, 236, 233
Irwin, J. B. 1952, ApJ, 116, 211
Kaitchuck, R. H., & Honeycutt, R. K. 1982, PASP, 94, 532
Kaitchuck, R. H., Honeycutt, R. K., & Schlegel, E. M. 1985, PASP, 97, 1178
Khaliullina, A. I. 2018, Astronomy Reports, 62, 520
Lampens, P., van Cauteren, P., Strigachev, A., et al. 2004, Information Bulletin on Variable Stars, 5572
Lanza, A. F. 2005, MNRAS, 364, 238
Lanza, A. F. 2006, MNRAS, 369, 1773
Lanza, A. F., & Rodonò, M. 1999, A&A, 349, 887
Li, Q. S., Zhai, D. S., Zhang, R. X., & Zhang, J. T. 1987, Acta Astrophysica Sinica, 7, 44
Liakos, A., Ulas, B., Gazeas, K., & Niarchos, P. 2008, Communications in Asteroseismology, 157, 336
Liao, W.-P., & Qian, S.-B. 2010, MNRAS, 405, 1930
Liao, W., Qian, S., Li, L., et al. 2016, Ap&SS, 361, 184
Mallama, A. D. 1980, ApJS, 44, 241
Martin, D. V., Mazeh, T., & Fabrycky, D. C. 2015, MNRAS, 453, 3554
Nijland, A. A. 1931, Astronomische Nachrichten, 242, 65
Perova, N. B. 1975, Peremennye Zvezdy, 20, 197
Qian, S. 2000a, AJ, 119, 901
Qian, S. 2000b, AJ, 119, 3064
Qian, S. 2001a, AJ, 121, 1614
Qian, S. 2001b, AJ, 122, 2686
Qian, S. 2002, MNRAS, 336, 1247
Qian, S. B., & Zhu, L. Y. 2002, ApJS, 142, 139
Samolyk, G. 2010, Journal of the American Association of Variable Star Observers (JAAVSO), 38, 85
Stewart, J. Q. 1915, ApJ, 42, 315
Tian, X.-M., Zhu, L.-Y., Qian, S.-B., et al. 2018, RAA (Research in Astronomy and Astrophysics), 18, 020

Todoran, I., & Popa, I. 1967, Information Bulletin on Variable Stars, 187
Tout, C. A., & Eggleton, P. P. 1988, MNRAS, 231, 823
Tout, C. A., & Hall, D. S. 1991, MNRAS, 253, 9
Vesper, D., Honeycutt, K., & Hunt, T. 2001, AJ, 121, 2723
Wang, Z.-H., & Zhu, L.-Y. 2016, New Astron., 49, 13
Wolf, G. W., & Kern, J. T. 1983, ApJS, 52, 429
Zasche, P., Liakos, A., Wolf, M., & Niarchos, P. 2008, New Astronomy, 13, 405
Zhang, J., Qian, S.-B., & Boonrucksar, S. 2009, Chinese Astronomy and Astrophysics, 33, 279
Zhu, L.-Y., Qian, S.-B., Zhou, X., et al. 2013, AJ, 146, 28
Zhu, L. Y., Qian, S. B., Zola, S., & Kreiner, J. M. 2009, AJ, 137, 3574
Zhu, L.-Y., Zhou, X., Hu, J.-Y., et al. 2016, AJ, 151, 107